HHS Public Access

Author manuscript

Sci Transl Med. Author manuscript; available in PMC 2016 April 15.

Published in final edited form as:

Sci Transl Med. 2015 April 15; 7(283): 283ra51. doi:10.1126/scitranslmed.aaa4442.

PI3K inhibition results in enhanced estrogen receptor function and dependence in hormone receptor-positive breast cancer

Ana Bosch[1,*], **Zhiqiang Li**[1], **Anna Bergamaschi**[2], **Haley Ellis**[1], **Eneda Toska**[1], **Aleix Prat**[3,4], **Jessica J. Tao**[5], **Daniel E. Spratt**[6], **Nerissa T. Viola-Villegas**[6,†], **Pau Castel**[1], **Gerard Minuesa**[7], **Natasha Morse**[1], **Jordi Rodón**[8,9], **Yasir Ibrahim**[10], **Javier Cortes**[8], **Jose Perez-Garcia**[8], **Patricia Galvan**[3], **Judit Grueso**[10], **Marta Guzman**[10], **John A. Katzenellenbogen**[11], **Michael Kharas**[7], **Jason S. Lewis**[6,7], **Maura Dickler**[12], **Violeta Serra**[10], **Neal Rosen**[7], **Sarat Chandarlapaty**[1,12,13], **Maurizio Scaltriti**[1], and **José Baselga**[1,12,13]

[1]Human Oncology & Pathogenesis Program (HOPP) and Memorial Sloan Kettering Cancer Center, 1275 York Avenue, Box 20, New York, NY 10065

[2]Department of Molecular and Integrative Physiology, University of Illinois at Urbana-Champaign, 524 Burrill Hall, Urbana 61801, IL, USA

[3]Translational Genomics Group, Vall d'Hebron Institute of Oncology (VHIO), Passeig Vall d'Hebron 119-129, Barcelona 08035, Spain

[4]Translational Genomics and Targeted Therapeutics in Solid Tumors, August Pi i Sunyer Biomedical Research Institute (IDIBAPS), Hospital Clinic Barcelona, C/Rosselló 149-153, Barcelona 08035, Spain

[5]Massachusetts General Hospital Cancer Center and Harvard Medical School, 425 13th street, Charlestown, MA 02129

[6]Department of Radiology at Memorial Sloan Kettering Cancer Center, New York, NY 10065

To whom correspondence should be addressed: Sarat Chandarlapaty, M.D., Ph.D., Memorial Sloan Kettering Cancer Center, Human Oncology & Pathogenesis Program (HOPP) and Department of Medicine, 1275 York Avenue, Box 20, New York (NY) 10065, Phone: +1 212-639-8000;, chandars@mskcc.org. Maurizio Scaltriti, Ph.D., Memorial Sloan Kettering Cancer Center, Human Oncology & Pathogenesis Program (HOPP), 1275 York Avenue, Box 20, New York (NY) 10065, Phone: +1 212-639-8000;, scaltrim@mskcc.org. José Baselga, M.D., Ph.D., Memorial Sloan Kettering Cancer Center, Human Oncology & Pathogenesis Program (HOPP) and Department of Medicine, 1275 York Avenue, New York (NY) 10065, Phone: +1 212-639-8000;, baselgaj@mskcc.org.

[*]Division of Oncology and Pathology, Department of Clinical Sciences, Lund University, Medicon Village Building 404:C2, Scheelevägen 2, SE-223 81 Lund, Sweden.

[†]Karmanos Cancer Institute, Department of Oncology, 4100 John R. Street, Detroit, MI, 48201, USA.

Author contributions: A.B., S.C., M.S., and J.B. designed the research. A.B., Z.L., H.E., E.T., J.T., P.C., G.M., and N.M., performed the experiments. A. Be. analyzed microarray gene expression data and performed GSEA. D.E.S., N.T.V. and J.K. performed and analyzed ^{18}F-FES-PET imaging. J.R., V.S., J.C., J. PG., and M.D. collected the human specimens. P.G. and A.P. performed and analyzed mRNA nCounter-gene expression procedure. V.S., Y.H.I., J.G. and M.G. established and performed experiments with PDXs. J.K., M.K., J.S.L and N.R. assisted with research design. A.B. prepared the figures. A.B., S.C., M.S., and J.B. wrote the manuscript.

Competing interests: J.B. and N.R. have consulted for Novartis Pharmaceuticals. J.B. is a past member of the scientific advisory board of Seragon. N.R. serves on advisory boards for AstraZeneca and Millennium. J.C. serves as an advisor for Roche/Genentech and has received speaking fees from Novartis and Roche. A.P. has served in an advisory role for Nanostring Technologies, Inc. J.R. serves on advisory boards for Novartis, Lilly, Leti, Servier, and KPS.

Data and material availability: BAY 80-6946 was kindly provided by Bayer (MTA SK2014-1248). 16α-^{18}F-fluoro-17β-estradiol (^{18}F-FES) was provided by the Radiochemistry and Molecular Imaging Probes Core Facility at MSKCC. Requests for materials will be accommodated with material transfer agreements (MTAs). Raw gene expression data for cell lines and xenografts were deposited in Gene Expression Omnibus (GSE64033). Raw gene expression data for patient samples were also deposited in Gene Expression Omnibus (GSE63579).

[7]Molecular Pharmacology and Chemistry Program and Center for Cell Engineering Memorial Sloan Kettering Cancer Center, New York, NY 10065

[8]Medical Oncology, Vall d'Hebron Institute of Oncology (VHIO), Passeig Vall d'Hebron 119-129, Barcelona 08035, Spain

[9]Universitat Autonoma de Barcelona, Plaza Cívica, Campus UAB, 08193

[10]Experimental Therapeutics Group, Vall d'Hebron Institute of Oncology, Passeig Vall d'Hebron 119-129, Barcelona 08035, Spain

[11]Department of Chemistry, University of Illinois at Urbana-Champaign, 524 Burrill Hall, Urbana 61801, IL, USA

[12]Breast Medicine Service, Department of Medicine, Memorial Sloan Kettering Cancer Center, 1275 York Avenue, Box 20, New York, New York 10065, USA

[13]Weill Cornell Medical College New York, NY 10065, USA

Abstract

Activating mutations of *PIK3CA* are the most frequent genomic alterations in estrogen receptor (ER)-positive breast tumors, and selective PI3Kα inhibitors are in clinical development. The activity of these agents, however, is not homogeneous, and only a fraction of patients bearing *PIK3CA*-mutant ER-positive tumors benefit from single agent administration. Searching for mechanisms of resistance, we observed that suppression of PI3K signaling results in induction of ER-dependent transcriptional activity, as demonstrated by changes in expression of genes containing ER binding sites and increased occupancy by the ER of promoter regions of upregulated genes. Furthermore, expression of *ESR1* mRNA and ER protein were also increased upon PI3K inhibition. These changes in gene expression were confirmed *in vivo* in xenografts and patient-derived models and in tumors from patients undergoing treatment with the PI3Kα inhibitor BYL719. The observed effects on transcription were enhanced by the addition of estradiol and suppressed by the anti-ER therapies fulvestrant and tamoxifen. Fulvestrant markedly sensitized ER-positive tumors to PI3Kα inhibition, resulting in major tumor regressions in vivo. We propose that increased ER transcriptional activity may be a reactive mechanism that limits the activity of PI3K inhibitors, and that combined PI3K and ER inhibition is a rational approach to target these tumors.

Introduction

The phosphatidylinositol 3-kinase (PI3K) pathway is essential for cell growth, proliferation, survival, and metabolism (1,2). The PI3K family of enzymes is divided into three main classes (I to III), with class I being the most often implicated in human cancer (3). Members of the class IA PI3K are characterized by a heterodimer composed of a catalytic subunit (p110α, β, and δ) and a regulatory subunit (p85) (4,5). *PIK3CA*, the gene coding for p110α, is frequently mutated in human cancers (6,7). In particular, hot spot mutations of this gene that reside in the helical (E542K and E545K) or catalytic (H1047R) domains are found in over a third of estrogen receptor (ER)-positive breast cancer, representing the most common genomic alteration in this group of tumors (7,8).

Selective PI3K p110α (PI3Kα) inhibitors are currently being tested in the clinic in patients with advanced malignancies, with promising results in patients with breast tumors harboring *PIK3CA* mutations (9,10). However, not all the patients benefit equally from these agents, and even those that initially respond typically relapse after months of therapy.

Although we have recently reported that the emergence of resistant clones with genomic alterations that activate PI3Kβ may partially explain acquired resistance to PI3Kα inhibitors (11), alternative mechanisms may also be at play in primary or early resistance to these therapies. Among them, activation of alternative cellular compensatory pathways could explain primary resistance or the emergence of rapid resistance. For example, we have shown that pharmacological suppression of mammalian target of rapamycin (mTOR), which is downstream from PI3K and a central node within the PI3K/AKT/mTOR axis, results in activation of both AKT (12) and ERK (13), and can account for decreased efficacy of mTOR inhibitors. Similarly, inhibition of PI3K leads to compensatory activation of upstream receptor tyrosine kinases that limit the effectiveness of these compounds (14,15).

Given that the vast majority of *PIK3CA*-mutant tumors are ER-positive, it is plausible to hypothesize that both pathways can drive proliferation and survival in these cells. A tangible evidence that the PI3K and ER pathways can cooperate in tumor progression came from a clinical study (16) that showed an impressive improvement in progression-free survival (PFS) in ER-positive breast cancer patients treated with the mTOR inhibitor everolimus in combination with the anti-estrogen aromatase inhibitor exemestane. These patients had failed prior endocrine therapy, and considering that activity of single agent mTOR inhibitors is minimal, these results suggest a synergistic activity in targeting mTOR and ER signaling simultaneously. Nevertheless, little is known about the reciprocal regulation of these key pathways, although it has been described that chronic anti-estrogen therapy induces the activation of the PI3K pathway *in vitro* (17,18). Perhaps more relevant to our interest in understanding the effects of PI3K inhibition on ER signaling, studies in prostate cancer have convincingly shown that the PI3K pathway regulates androgen receptor activity (19).

Based on all these observations, our work was aimed at studying the effects of PI3Kα inhibition on ER signaling and at deciphering its potential effect on limiting the efficacy of PI3K inhibitors. We report that inhibition of the PI3K pathway triggers the activation of the ER-dependent transcription machinery. The importance of this adaptive response is underscored by the finding that suppression of ER activity can sensitize tumors to PI3K inhibition.

Results

PI3K inhibition promotes ER activity

To obtain a comprehensive view of the role of PI3K activation in modulating ER function, we examined the effects of pharmacological PI3K inhibition in ER-positive breast cancer cells that harbor activating *PIK3CA* mutations (MCF7-*E545K*, T47D-*H1047R*). Previous studies have established that a large portion of the transcriptome in these cells is regulated by ER activity (20), so they were a good model to explore whether PI3K inhibition had any effect on ER-regulated genes. Cells were treated with the highly selective PI3Kα inhibitor

BYL719 at 1 μM for 4, 8, 12, 24, or 48 hours, and cellular lysates were analyzed. As measured by intensity of phosphorylation of AKT (S473) and S6 (S235/6), BYL719 caused potent inhibition of PI3K signaling as early as 4 hours after drug exposure and lasting for 48 hours, with a slight rebound in activity observed at the 48 hour time point (fig. S1).

We observed that at this concentration BYL719 also induced global changes in the transcription profile of both MCF7 and T47D cells. Perturbations in their gene expression profiles were evident 12 hours after the addition of BYL719 to the culture media, and were sustained until at least 48 hours (Fig. 1A and fig. S2, respectively). Strikingly, of the 383 and 706 genes significantly altered upon BYL719 treatment in MCF7 and T47D cells (FDR ≤ 1%), respectively, up to 60% contained an estrogen responsive element (ERE) in their promoter (Fig. 1B). Gene Set Enrichment Analysis (GSEA) was conducted on the genes altered by PI3K inhibition and demonstrated that gene sets characterized by ER dependence were highly enriched in this group (FDR ≤ 25%) (Fig. 1C, fig. S3, and table S1). Based on these findings, we next decided to confirm the relationship between PI3K activity and ER transcriptional activity by analyzing the effects of drug inhibition on promoters known to be stimulated by estrogen. First, we examined the effect of BYL719 treatment on expression of a luciferase transgene linked to a 3X-ERE promoter. Sixteen hours after treatment, an approximately 2-fold higher luminescence was detected in the BYL719-treated cells than the DMSO-treated cells (Fig. 1D).

We next used PCR to confirm that drug treatment had an effect on the expression of endogenous mRNAs known to be regulated by ER, including progesterone receptor (*PGR*), growth regulation by estrogen in breast cancer 1(*GREB1*), and insulin-like growth factor binding protein 4 (*IGFBP4*) (Fig. 1E). The increased expression was due, at least in part, to ER transcriptional activity, because ChIP-qPCR experiments showed a 2–3 fold enhancement in occupancy by ER of the promoter regions of these upregulated genes (Fig. 1F). Taken together, our findings demonstrate that inhibition of activated PI3K signaling present in *PIK3CA*-mutant ER-positive breast cancer cells is associated with an increase in the transcriptional function of the ER.

In addition to *PIK3CA* mutations, there are other genetic mechanisms that also result in aberrant PI3K pathway signaling. Specifically, PTEN function is lost in a subset of ER-positive tumors (21). Unlike *PIK3CA* mutation, PTEN loss appears to activate PIP3/AKT signaling preferentially through the p110β subunit, and PI3Kα selective inhibitors do not inhibit PI3K/AKT signaling in these cells (22). Because AKT is downstream from PI3K, we used MK2206, a selective AKT inhibitor, in CAMA1 cells ($PTEN^{mut}$ D92H) (fig. S4) to test whether inhibition of the PI3K pathway promoted ER activation in an ER-positive *PTEN*-mutant model. Similar to MCF7 and T47D cells treated with BYL719, suppression of AKT in CAMA1 cells resulted in an overall increased expression of ER-dependent genes and in the induction of an ER-dependent signature (fig. S5 and table S2). The activation of ER as a consequence of PI3K pathway inhibition in the context of $PTEN^{null/mut}$ tumors was further corroborated by assessing the effect of the AKT inhibitor MK2206 upon *PGR* and *GREB1* expression by qPCR in CAMA1, ZR-75-1, and MDA-MB-415 cells (fig. S6). Overall, the findings observed in both *PTEN* and *PIK3CA*-mutant ER-positive breast cancer models are

similar and demonstrate an increased ER-dependent transcription activity upon inhibition of the PI3K pathway by different strategies.

PI3K inhibition increases ER expression

As mentioned above, we found that inhibition of PI3K promotes ER activity, as manifested by increases in ER binding to target promoters and increases in ER target gene expression. We speculated that ER expression itself might also be increased in response to PI3K inhibition and might partially explain the increases in ER activity. We examined *ESR1* mRNA expression in a panel of ER-positive breast cancer cell lines (Fig. 2A and B and fig. S7) and found increases ranging from 1.5x-3x upon PI3K inhibition with BYL719, with maximal accumulation observed at 24 hours in the MCF7 model. Coinciding with the initial rise in mRNA (8 hours), RNA Polymerase II binding to the *ESR1* promoter was observed to be increased approximately 2 fold by ChIP assay (fig. S8). A similar induction of the *ESR1* transcript was observed with various PI3K inhibitors (GDC0032, GDC0941, BAY80-6946, and BKM120) in ER-positive/*PIK3CA* mutant models (fig. S9). The increase in *ESR1* mRNA coincided with increases in the ER protein, which was also maximal at approximately 24 hours over a 48 hour time course (Fig. 2B). Comparing the effects of PI3K inhibition with mTORC1 inhibition on *ESR1* regulation, we observed an appreciable increase in the expression of *ESR1* and its target genes also during rapamycin treatment, albeit with a lower magnitude compared to BYL719 (fig. S10). Together, the data show an increase in ER expression as a result of PI3K inhibition in various cell culture systems. To determine if increases in ER expression and activity might be observed *in vivo*, we used a non-invasive probe of ER expression, 16α-^{18}F-fluoro-17β-estradiol Positron Emission Tomography (^{18}F-FES-PET). This probe measures uptake of labeled estradiol as an indirect measure of ER expression. In T47D xenografts, we observed a selective increase in tumor uptake of ^{18}F-FES in mice treated with BYL719 compared to those receiving vehicle (Fig. 2C). Although such differences could be due to other mechanisms, such as changes in tumor retention time or receptor affinity for estradiol, they are consistent with the findings of increased expression of the receptor observed *in vitro* (Fig. 2A and B, fig. S7–S9)

To assess the clinical relevance of our findings, we analyzed the gene expression profiles of tumor samples collected from patients treated with BYL719 as part of either the first-in-human clinical trial (9) or an ongoing clinical study testing the efficacy of BYL719 in combination with the aromatase inhibitors letrozole or exemestane (NCT01870505). Paired tumor biopsies were collected from patients before commencing BYL719 therapy and after a minimum of 14 days on treatment, between four and six hours after the daily drug administration. Two patients were treated with BYL719 as a single agent, and eight patients were treated with the combination of BYL719 and an aromatase inhibitor. Table S3 shows the patients' information, including breast tumor histology at diagnosis, *PIK3CA* mutation status, BYL719 dose, and the treatment in combination with BYL719 (if any). Of note, either as single agent or in combination, BYL719 was administered at clinically active doses in all cases (11,23).

The expression of 105 breast cancer-related genes, including the genes from the PAM50 intrinsic subtype predictor (24), was compared across the twenty paired biopsies. Thirty-nine

genes were differentially expressed (FDR ≤ 25%; table 1). Not surprisingly, proliferation-related genes such as *MKI67*, *BIRC5*, and *CENPF* were among the most highly down-regulated genes in the on-treatment samples, whereas the anti-apoptotic genes *BCL2* and *MDM2* were up-regulated. Central to our work, *ESR1* and its target gene *PGR* were among the most highly induced genes upon PI3K inhibition (table 1). The *ESR1* transcript levels were shown to increase during PI3K inhibition in all but two patients evaluated (Fig. 2D). In accordance with this result, a switch from a non-Luminal A phenotype (Luminal B or HER2-enriched) in the pre-treatment sample to a Luminal A subtype in the on-treatment sample was identified by the PAM50 subtype predictor in three (Patients 1, 4, and 6) of the six patients (Patients 1, 3, 4, 6, 9, and 10) who showed the highest increase in *ESR1* (table S3). There was a global shift in the transcriptional profile of the tumors towards a more luminal A-like signature across all “on-treatment” samples (Fig 2E). Of note, the pre-treatment sample from Patient 2 was already identified as Luminal A; however, we observed a higher expression of the Luminal A signature in the on-treatment sample compared to the pre-treatment sample. Furthermore, Patient 9 presented a change in intrinsic subtype from basal-like in the pre-treatment sample to luminal B in the on-treatment biopsy, which was accompanied by the highest increase in *ESR1* expression (Figs. 2D and 2E). Although these are small numbers of patients, the data support the idea that ER mRNA increases upon PI3K inhibition, in conjunction with a more estrogen-dependent luminal-A phenotype.

In an attempt to identify the mechanisms responsible for the observed increase in *ESR1* transcription upon PI3Kα inhibition, we hypothesized that the expression and/or activity of transcription factors known to bind the promoter of *ESR1* were augmented under these conditions. As such, we investigated the possible role of FOXO3A, a transcription factor known to be regulated by PI3K/AKT signaling, in regulating ER expression. We found that inhibition of PI3K with BYL719 led to a >5x accumulation of FOXO3A at the ESR1 promoter by ChIP assay (Fig 2F). To determine if the induction of FOXO3A binding was necessary for the increase in ESR1 mRNA, we used siRNA to knock down FOXO3A in MCF7 cells and found that the loss of FOXO3A prevented the induction of ESR1 caused by BYL719 (Fig 2G). These data suggest that FOXO3A is necessary for the effect of PI3K inhibition upon ESR1 expression.

PI3K inhibition-induced ER activity is enhanced by the presence of ligand

The effects of ER on breast cancer progression are thought to be dependent upon both ligand-dependent and ligand-independent mechanisms (25,26). Because these different modes of activation have implications for the optimal means of pharmacologic inhibition of ER, we investigated whether the induction of ER activity required the presence of estradiol (E2). MCF7 cells were grown in medium depleted of steroidal hormones (CSS) for 48 hours and then treated with DMSO (vehicle), BYL719, E2, or the combination of BYL719 and E2 for 4 hours, and ChIP assays were performed. As expected, the addition of estradiol increased ER binding to the *PGR* and *GREB1* promoters approximately 3 fold compared to control cells not exposed to E2. In the presence of E2, 1 μM BYL719 caused further enhancement of binding 2–3 fold over E2 alone (Fig. 3A and B). However, in the absence of E2, BYL719 caused a much smaller enhancement of binding (1.2–1.5x) over untreated cells. Similarly, when we examined the effect of PI3K inhibition on transcription of *PGR* and

GREB1, we again found that addition of E2 or the combination of E2 and BYL719 promoted *PGR* and *GREB1* accumulation. However, BYL719 treatment in the absence of E2 caused very little increase in *PGR* or *GREB1* after 0 to 16 hours of drug exposure (Fig. 3C).

We next analyzed the effects of the ER antagonists, 4-hydroxy-tamoxifen (4-OHT) and fulvestrant by qPCR. Under normal serum conditions, both 4-OHT (1 μM) and fulvestrant (100 nM) attenuated the expression of ER target genes with no impact on *ESR1* mRNA (fig. S11). The same inhibitors were sufficient to prevent BYL719-mediated increased expression of the four tested ER target genes (Fig. 3D and fig. S12). These data suggest that blockade of estrogen function mitigates the effects mediated by PI3K inhibition.

PI3K inhibition in combination with ER-inhibitor fulvestrant has profound antitumor activity in ER/PIK3CA^{mut} models

Because fulvestrant was the most potent antagonist of PI3K inhibitor-induced ER activity, we chose to use this agent to characterize the biologic consequences of the ER induction. We used two well-established ER-positive/*PIK3CA*^{mut} xenograft models (MCF7 and T47D cells) to test the combination. Daily administration of BYL719 (25 mg/kg) resulted in modest reduction of tumor growth in both models (Fig. 4A and fig. S13). Fulvestrant monotherapy (200 mg/Kg biw) was sufficient to prevent further tumor growth and, in some cases, to induce tumor shrinkage. However, the combination of both agents showed marked tumor regression and in some cases resulted in complete tumor remissions. Consistent with a tumor cell-autonomous effect of the combination, fulvestrant and BYL719 in combination potently inhibited cell cycle progression in MCF7 cells *in vitro* (fig. S14). Not only were these effects seen in cell line-derived xenograft models, but also when we further investigated the effects of these treatments in a patient-derived xenograft (PDX) model of ER-positive *PIK3CA*^{mut} (H1047R) breast cancer (Fig. 4B). Of note, this PDX was established from a patient who had previously progressed on multiple lines of endocrine therapy, including fulvestrant. In this model, the combination of BYL719 and fulvestrant induced partial tumor regression, despite very limited single agent activity for either BYL719 or fulvestrant. To confirm that the lack of tumor regressions from single agent BYL719 was not due to failure of the drug to inhibit the target in vivo, we collected a set of MCF7 xenografts for analysis after 4 days of treatment. BYL719 effectively inhibited pAKT (S473), as well as phosphorylation of the ribosomal protein S6, a downstream effector of S6K, indicative of a therapeutic dose of BYL719 (Fig. 4C). Moreover, ER protein expression showed a marked increase with BYL719 treatment that was mitigated by the addition of fulvestrant.

Finally, to confirm our observations that ER activity is induced by the PI3K inhibitor *in vivo*, gene expression analysis was conducted on a representative cohort of the PDX and MCF7 xenografts. Tumors were collected after short-term treatment (4–7 days), and gene expression profiling revealed that BYL719 significantly varied the expression of 190 genes (FDR ≤ 1%) in the PDX models, 61% of which have an ER binding site in their promoter (Fig. 4D). This translated to enrichment for an ER-dependent signature, as confirmed with GSEA (Fig. 4E). A similar enrichment in the ER-dependent signature was seen in the treated

MCF7 tumors (Fig. 4F). Taken together, these data indicate that the increase in ER expression and function mediated by PI3K suppression attenuates the benefit of the PI3K inhibitor and strongly suggests that combinations of PI3K and ER inhibitors should be tested in the clinic.

Discussion

In this work, we show that inhibition of the PI3K pathway in ER-positive breast cancer results in induction of ER-dependent transcriptional activity. These effects on the transcriptome were not restricted to a few selected ER target genes, but rather expression of hundreds of genes controlled by ERE-containing promoters. The causative role of ER in rewiring gene expression upon PI3K inhibition was underscored by its complete prevention when fulvestrant, a direct ER antagonist, was added to the system.

These observations led us to consider whether one of the mechanisms for up-regulation of ER signaling was augmentation of ER itself. This indeed proved to be the case, and we found a consistent increase in ER transcript and induction of a luminal signature (typical of hormone-responsive breast cancers) in cell lines, murine models, and patient samples upon suppression of the PI3K pathway. However, it remains to be elucidated whether this increase in ER expression is the sole factor responsible for the induction of ER activity after PI3K inhibition. This increase in ER transcription is likely to be an adaptive response to the inhibition of the PI3K pathway. Indeed, we and others have shown that non-genetic activation of compensatory pathways is frequently observed in response to a variety of targeted therapies and it may limit their efficacy (12–15). We surmise that the compensatory activation of ER-dependent genes occurring early upon PI3K inhibition decreases the antitumor efficacy of PI3K inhibitors. This may explain the limited activity of PI3K inhibitors when used as monotherapy in patients with ER-positive breast cancer and suggests that simultaneous ER suppression would be a logical strategy to combine with PI3K inhibition. The clinical activity observed in ER-positive patients treated with the combination of the mTOR inhibitor everolimus and an aromatase inhibitor (16), as well as very early clinical data with PI3Kα inhibitors in combination with other anti-estrogen agents (27–29) seem to support this hypothesis. Consistent with our PDX data, these clinical studies indicate that dual PI3K and ER blockade is effective even in patients who had progressed on previous anti-estrogen therapies.

We are aware that our findings have certain limitations. We have not tested the ligand-dependency of ER in vivo, mainly because of a lack of preclinical models of aromatase inhibition, a standard of care in post-menopausal women. Moreover, we acknowledge that the clinical validation of our findings would benefit from a larger cohort of patients treated with PI3K inhibitors than the one used in this work. The requirement of paired pre-treatment and on-treatment samples to study acute changes in gene expression, however, limits the number of patients suitable for these analyses. This is a caveat that should be taken into consideration at the time of designing clinical trials, where mandatory on-treatment biopsies could provide important information on early adaptive response to therapy.

Reflecting on our findings, one cannot escape from drawing a parallel with prostate cancer, where a reciprocal feedback regulation of PI3K and androgen receptor (AR) activity has been recently described (19). In the case of prostate cancer, inhibition of the PI3K pathway results in activation of AR and, conversely, blockade of AR activates PI3K signaling. This bidirectional crosstalk seems to also occur in the breast where, in addition to our findings showing ER activation upon PI3K inhibition, inactivation of ER appears to be associated with activation of PI3K signaling (18,30). This speaks for a true interdependency between these two pathways, where a state of equilibrium between PI3K and ER signaling is reached to ensure cell survival. Thus, both prostate and breast cancer cells may adapt to suppression of the PI3K pathway by increasing their dependence on the hormone receptor function.

In our hands, ER degradation by fulvestrant treatment was more effective than the ER modulator 4-OH-tamoxifen for re-sensitizing tumors to PI3K inhibitors. A plausible explanation for these results is that ER degradation may potentially prevent both the estrogen-dependent and estrogen-independent activity (31,32) mediated by PI3K inhibition. However, further studies will be required to confirm which of the currently available anti-estrogen therapies, if any, is superior when given in combination with PI3K inhibitors.

In summary, our results suggest that PI3K blockade in ER-positive breast cancer triggers an ER-dependent transcriptional program that ultimately may be reversed with ER targeting therapies. Thus, simultaneous blockade of PI3K and ER may be needed for optimal treatment of ER-positive breast tumors with aberrant activation of the PI3K pathway.

Materials and Methods

Study Design

The aim of our study was to explore the mechanism by which the combination of PI3K pathway inhibitors and estrogen receptor function blockade results in superior antitumor activity. We aimed to evaluate whether changes in ER function were influencing the clinical response to anti-PI3K therapy in ER-positive breast tumors that harbor PI3K pathway activation. For this purpose, we planned to use various specific PI3K inhibitors, namely: BYL719 (p110α specific catalytic inhibitor), GDC0941, and BKM120 (pan-PI3K inhibitors), GDC0032 and BAY80-6946 (p110β sparing PI3K inhibitors) in a panel of ER-positive breast cancer cell lines and xenografts that harbor *PIK3CA* activating mutations. We also used MK2206 (pan-AKT allosteric inhibitor) to inhibit the PI3K pathway in ER-positive cell lines which activate this pathway through PTEN loss. Finally, to evaluate the role of ER up-regulation as a pro-survival signal in our *in vitro* and *in vivo* models, we planned to use the selective ER modulator 4-hydroxy-tamoxifen (4-OHT) and degrader fulvestrant. For the *in vivo* experiments, the number of animals in each group was calculated to measure a 25% difference between the means of placebo and treatment groups with a power of 80% and a *p* value of 0.01. Host mice carrying xenografts were randomly and equally assigned to either control or treatment groups. Animal experiments were conducted in a controlled and non-blinded manner. We also used RNAseq to evaluate gene expression changes in breast cancer patients who underwent BYL719-based therapy to validate our *in vitro* findings on ER expression.

In vitro experiments were performed at least two times and at least in triplicate.

Plasmids

pRL-TK *Renilla* Luciferase plasmid was obtained from Promega, and 3×-ERE-TATA-Luciferase reporter was obtained from Addgene (plasmid 28230 deposited by Donald McDonnell (33)).

Establishment of tumor xenografts and in vivo treatments

All mouse studies were conducted through Memorial Sloan Kettering Cancer Center, Massachusetts General Hospital Cancer Center, and Vall d'Hebron Institute of Oncology Institutional Animal Care and Use Committees (IACUC) approved animal protocols in accordance with institutional guidelines. Six-week-old female athymic nude mice were purchased from Charles River Laboratories and housed in air-filtered laminar flow cabinets with a 12-hour light cycle and food and water *ad libitum*. The size of the animal groups was calculated to measure a difference of means of 25% between placebo and treatment groups with a power of 80% and a p value of 0.01. Host mice carrying xenografts were randomly assigned to either control or treatment groups. Animal experiments were conducted in a non-blinded manner. For cell line-derived xenograft studies, mice were injected subcutaneously with $1X10^7$ MCF7 or T47D suspended in 150 μL culture medium/Matrigel (BD Biosciences) in a 1:1 ratio. For PDXs, patient consent for tumor use in animals was obtained under a protocol approved by the Vall d'Hebron Hospital Clinical Investigation Ethical Committee and Animal Use Committee. PDXs were derived from a ER-positive PR-positive HER2-negative breast cancer patient previously treated with both chemotherapy (taxanes and vinorelbine) and anti-endocrine therapy (exemestane and fulvestrant). Tumors (~2×2 mm size) were subcutaneously implanted in 6 week old female HsdCpb:NMRI-*Foxn1nu* mice (Harlan Laboratories).

All animals were supplemented with 1 μM 17β-estradiol (Sigma) in their drinking water One μmol/L of 17β-estradiol was added to the mouse drinking water as described (34).

Once tumors reached an average volume of ~75–250 mm^3, mice were randomized into treatment arms, with n=7–10 tumors/group. BYL719 was dissolved in 0.5% carboxymethylcellulose solution and administered once daily via oral gavage at 25 mg/kg. Fulvestrant was diluted in castor oil and administered subcutaneously twice weekly (biw) at 200 mg/kg. Tumors were measured by digital caliper twice per week over the entire treatment period and, where indicated, harvested 2 hours after the last drug administration. Tumor volume was determined using the formula: $(\text{length} \times \text{width}^2) \times (\pi/6)$. Tumor volumes are plotted as means ± SEM.

mRNA nCounter-gene expression procedure

A section of the formalin-fixed paraffin-embedded (FFPE) breast tissue was first examined with hematoxylin and eosin staining to determine the tumor surface area and cellularity. For RNA purification (Roche High Pure FFPET RNA isolation kit), 1 to 3 10 μm FFPE slides were cut for each tumor, and macrodissection was performed, when needed, to avoid normal breast contamination. A minimum of ~100 ng of total RNA was used to measure the

expression of 105 breast cancer-related genes and 5 house-keeping genes using the nCounter platform (Nanostring Technologies) (37). Data were log base 2 transformed and normalized using 5 house-keeping genes (ACTB, MRPL19, PSMC4, RPLP0, and SF3A1). Raw gene expression data for patient samples were deposited in Gene Expression Omnibus (GSE63579). The list of 105 genes includes genes from the following 3 signatures: PAM50 intrinsic subtype predictor (n=50) (24), Claudin-low subtype predictor (n=43) (38), and 13-VEGF/Hypoxia signature (n=13)(39). In addition, we included 8 individual genes that have been found to play an important role in breast cancer (CD24, CRYAB, ERBB4, PIK3CA, PTEN, RAD17, RAD50, and RB1).

All tumors were assigned to an intrinsic molecular subtype of breast cancer (Luminal A, Luminal B, HER2-enriched, Basal-like or the Normal-like group) using the previously reported PAM50 subtype predictor (24).

Analyses of microarray and mRNA nCounter-gene expression data

Illumina IDAT files were preprocessed using the IlluminaExpressionFileCreator module on GenePattern (http://www.broad.mit.edu/cancer/software/genepattern). Supervised analysis to find genes associated with PI3K pathway inhibition treatments was performed using Significance Analysis of Microarrays (SAM) (40). The multi-class unpaired or the two-class paired method of SAM were used to identify genes whose expression differed significantly among treatments and/or time points. False discovery rate (FDR) was set as less than or equal to 1% for microarray-based analysis or to 25% for nCounter-based analysis. Gene Set Enrichment Analysis (GSEA) was used to determine the extent to which expression profiles were enriched for *a priori* defined sets of genes from biologically coherent pathways (41). Gene set enrichment analysis (GSEA) was performed using version 2.0 of GSEA run on all the gene sets in version 2.5 of the Molecular Signatures Database (MSigDB) and to correct for multiple hypotheses testing; the FDR threshold was set at ≤ 0.25. A list of the specific signatures used for graphical representation and their specific description has been added to the Excel file with raw data (table S4).

Statistical analysis

Statistical analysis for *in vitro* and *in vivo* experiments was performed using GraphPad Prism (GraphPad Software). When comparing two groups (control vs. treated), two-tailed Student's unpaired *t* test was performed (significance level set at $p<0.05$). When comparing various groups, one-way ANOVA statistical test was used, applying the Bonferroni method to correct for multiple comparisons. Independent experiments were conducted with a minimum of two biological replicates per condition to allow for statistical comparison. Error bars represent the standard error of the mean (SEM), *p* values are indicated. All cellular experiments were repeated at least two times. For ChIP analysis (Fig. 1F), the data are presented as fold-enrichment relative to *βActin* as a control gene region. Error bars represent SEM of three independent experiments. For the ChIP analyses in Fig. 2G, 3A and B, and fig. S8, data were normalized to their respective input signals and thus represented as %input. Two-tailed Student's unpaired *t* test was performed ($p<0.05$) comparing control vs. treated samples. Error bars represent the SEM of at least two independent experiments. Raw data for the figures are provided in table S4.

Supplementary Material

Refer to Web version on PubMed Central for supplementary material.

Acknowledgments

Funding: This work was funded by a Stand Up To Cancer Dream Team Translational Cancer Research Grant, a program of the Entertainment Industry Foundation (SU2C-AACR-DT0209 to J.B.), the Breast Cancer Research Foundation (to J.B.), the European Research Council (AdG09250244 to J.B.), the Instituto de Salud Carlos III (Intrasalud PSO9/00623 to J.B.) and Banco Bilbao Vizcaya Argentaria (BBVA) Foundation (Tumor Biomarker Research Program). A.B. holds a Translational Research Fellowship from the Spanish Society of Medical Oncology (SEOM). V.S. is a recipient of an Instituto de Salut Carlos III grant (FIS PI13/01714) and a GHD/FERO Grant. SC receives research funding from a Louis Gerstner YIA and the Damon Runyon Foundation. N.R. receives research funding from Bayer. N.T.V. held a K99/R00 Pathway to Independence award (1K99CA181492-01A1). J.A.K. was funded by PHS 5R01 CA 025836.

References and Notes

1. Engelman JA, Luo J, Cantley LC. The evolution of phosphatidylinositol 3-kinases as regulators of growth and metabolism. Nat Rev Genet. 2006; 7:606–619. [PubMed: 16847462]
2. Cantley LC. The phosphoinositide 3-kinase pathway. Science. 2002; 296:1655–1657. [PubMed: 12040186]
3. Engelman JA. Targeting PI3K signalling in cancer: opportunities, challenges and limitations. Nat Rev Cancer. 2009; 9:550–562. [PubMed: 19629070]
4. Brachmann SM, Ueki K, Engelman JA, Kahn RC, Cantley LC. Phosphoinositide 3-kinase catalytic subunit deletion and regulatory subunit deletion have opposite effects on insulin sensitivity in mice. Mol Cell Biol. 2005; 25:1596–1607. [PubMed: 15713620]
5. Zhao L, Vogt PK. Helical domain and kinase domain mutations in p110alpha of phosphatidylinositol 3-kinase induce gain of function by different mechanisms. Proc Natl Acad Sci U S A. 2008; 105:2652–2657. [PubMed: 18268322]
6. Kang S, Bader AG, Vogt PK. Phosphatidylinositol 3-kinase mutations identified in human cancer are oncogenic. Proc Natl Acad Sci U S A. 2005; 102:802–807. [PubMed: 15647370]
7. Samuels Y, Wang Z, Bardelli A, Silliman N, Ptak J, Szabo S, Yan H, Gazdar A, Powell SM, Riggins GJ, Willson JK, Markowitz S, Kinzler KW, Vogelstein B, Velculescu VE. High frequency of mutations of the PIK3CA gene in human cancers. Science. 2004; 304:554. [PubMed: 15016963]
8. Isakoff SJ, Engelman JA, Irie HY, Luo J, Brachmann SM, Pearline RV, Cantley LC, Brugge JS. Breast cancer-associated PIK3CA mutations are oncogenic in mammary epithelial cells. Cancer Res. 2005; 65:10992–11000. [PubMed: 16322248]
9. Juric D, Rodon J, Gonzalez-Angulo AM, Burris HA, Bendell J, Berlin JD, Middleton MR, Bootle D, Boehm M, Schmitt A, Rouyrre N, Quadt C, Baselga J. Abstract CT-01: BYL719, a next generation PI3K alpha specific inhibitor: Preliminary safety, PK, and efficacy results from the first-in-human study. Cancer Res. 2012; 72:CT-01.
10. Juric D, Krop I, Ramanathan RK, Xiao J, Sanabria S, Wilson TR, Choi Y, Parmar H, Hsu J, Baselga J, Von Hoff DD. Abstract LB-64: GDC-0032, a beta isoform-sparing PI3K inhibitor: Results of a first-in-human phase Ia dose escalation study. Cancer Res. 2013; 73:LB-64.
11. Juric D, Castel P, Griffith M, Griffith OL, Won HH, Ellis H, Ebbesen SH, Ainscough BJ, Ramu A, Iyer G, Shah RH, Huynh T, Mino-Kenudson M, Sgroi D, Isakoff S, Thabet A, Elamine L, Solit DB, Lowe SW, Quadt C, Peters M, Derti A, Schegel R, Huang A, Mardis ER, Berger MF, Baselga J, Scaltriti M. Convergent loss of PTEN leads to clinical resistance to a PI(3)Kalpha inhibitor. Nature. 2014; 518:240–244. [PubMed: 25409150]
12. O'Reilly KE, Rojo F, She QB, Solit D, Mills GB, Smith D, Lane H, Hofmann F, Hicklin DJ, Ludwig DL, Baselga J, Rosen N. mTOR inhibition induces upstream receptor tyrosine kinase signaling and activates Akt. Cancer Res. 2006; 66:1500–1508. [PubMed: 16452206]
13. Carracedo A, Ma L, Teruya-Feldstein J, Rojo F, Salmena L, Alimonti A, Egia A, Sasaki AT, Thomas G, Kozma SC, Papa A, Nardella C, Cantley LC, Baselga J, Pandolfi PP. Inhibition of

mTORC1 leads to MAPK pathway activation through a PI3K-dependent feedback loop in human cancer. J Clin Invest. 2008; 118:3065–3074. [PubMed: 18725988]

14. Serra V, Scaltriti M, Prudkin L, Eichhorn PJ, Ibrahim YH, Chandarlapaty S, Markman B, Rodriguez O, Guzman M, Rodriguez S, Gili M, Russillo M, Parra JL, Singh S, Arribas J, Rosen N, Baselga J. PI3K inhibition results in enhanced HER signaling and acquired ERK dependency in HER2-overexpressing breast cancer. Oncogene. 2011; 30:2547–2557. [PubMed: 21278786]
15. Chandarlapaty S, Sawai A, Scaltriti M, Rodrik-Outmezguine V, Grbovic-Huezo O, Serra V, Majumder PK, Baselga J, Rosen N. AKT inhibition relieves feedback suppression of receptor tyrosine kinase expression and activity. Cancer Cell. 2011; 19:58–71. [PubMed: 21215704]
16. Baselga J, Campone M, Piccart M, Burris HA 3rd, Rugo HS, Sahmoud T, Noguchi S, Gnant M, Pritchard KI, Lebrun F, Beck JT, Ito Y, Yardley D, Deleu I, Perez A, Bachelot T, Vittori L, Xu Z, Mukhopadhyay P, Lebwohl D, Hortobagyi GN. Everolimus in postmenopausal hormone-receptor-positive advanced breast cancer. N Engl J Med. 2012; 366:520–529. [PubMed: 22149876]
17. Miller TW, Balko JM, Fox EM, Ghazoui Z, Dunbier A, Anderson H, Dowsett M, Jiang A, Smith RA, Maira SM, Manning HC, Gonzalez-Angulo AM, Mills GB, Higham C, Chanthaphaychith S, Kuba MG, Miller WR, Shyr Y, Arteaga CL. ERalpha-dependent E2F transcription can mediate resistance to estrogen deprivation in human breast cancer. Cancer Discov. 2011; 1:338–351. [PubMed: 22049316]
18. Morrison MM, Hutchinson K, Williams MM, Stanford JC, Balko JM, Young C, Kuba MG, Sanchez V, Williams AJ, Hicks DJ, Arteaga CL, Prat A, Perou CM, Earp HS, Massarweh S, Cook RS. ErbB3 downregulation enhances luminal breast tumor response to antiestrogens. J Clin Invest. 2013; 123:4329–4343. [PubMed: 23999432]
19. Carver BS, Chapinski C, Wongvipat J, Hieronymus H, Chen Y, Chandarlapaty S, Arora VK, Le C, Koutcher J, Scher H, Scardino PT, Rosen N, Sawyers CL. Reciprocal feedback regulation of PI3K and androgen receptor signaling in PTEN-deficient prostate cancer. Cancer Cell. 2011; 19:575–586. [PubMed: 21575859]
20. Carroll JS, Meyer CA, Song J, Li W, Geistlinger TR, Eeckhoute J, Brodsky AS, Keeton EK, Fertuck KC, Hall GF, Wang Q, Bekiranov S, Sementchenko V, Fox EA, Silver PA, Gingeras TR, Liu XS, Brown M. Genome-wide analysis of estrogen receptor binding sites. Nat Genet. 2006; 38:1289–1297. [PubMed: 17013392]
21. N. Cancer Genome Atlas. Comprehensive molecular portraits of human breast tumours. Nature. 2012; 490:61–70. [PubMed: 23000897]
22. Wee S, Wiederschain D, Maira SM, Loo A, Miller C, deBeaumont R, Stegmeier F, Yao YM, Lengauer C. PTEN-deficient cancers depend on PIK3CB. Proc Natl Acad Sci U S A. 2008; 105:13057–13062. [PubMed: 18755892]
23. Elkabets M, Vora S, Juric D, Morse N, Mino-Kenudson M, Muranen T, Tao J, Campos AB, Rodon J, Ibrahim YH, Serra V, Rodrik-Outmezguine V, Hazra S, Singh S, Kim P, Quadt C, Liu M, Huang A, Rosen N, Engelman JA, Scaltriti M, Baselga J. mTORC1 inhibition is required for sensitivity to PI3K p110alpha inhibitors in PIK3CA-mutant breast cancer. Sci Transl Med. 2013; 5:196ra199.
24. Parker JS, Mullins M, Cheang MC, Leung S, Voduc D, Vickery T, Davies S, Fauron C, He X, Hu Z, Quackenbush JF, Stijleman IJ, Palazzo J, Marron JS, Nobel AB, Mardis E, Nielsen TO, Ellis MJ, Perou CM, Bernard PS. Supervised risk predictor of breast cancer based on intrinsic subtypes. J Clin Oncol. 2009; 27:1160–1167. [PubMed: 19204204]
25. Massarweh S, Osborne CK, Creighton CJ, Qin L, Tsimelzon A, Huang S, Weiss H, Rimawi M, Schiff R. Tamoxifen resistance in breast tumors is driven by growth factor receptor signaling with repression of classic estrogen receptor genomic function. Cancer Res. 2008; 68:826–833. [PubMed: 18245484]
26. Yamnik RL, Digilova A, Davis DC, Brodt ZN, Murphy CJ, Holz MK. S6 kinase 1 regulates estrogen receptor alpha in control of breast cancer cell proliferation. J Biol Chem. 2009; 284:6361–6369. [PubMed: 19112174]
27. Juric, D.; Saura, C.; Cervantes, A.; Kurkjian, C.; Patel, M.; Sachdev, J.; Mayer, I.; Krop, IE.; Oliveira, M.; Sanabria, S.; Cheeti, S.; Lin, RS.; Graham, RA.; Wilson, TR.; Parmar, H.; Hsu, JY.; Von Hoff, DD.; Baselga, J. Ph1b study of the PI3K inhibitor GDC-0032 in combination with

fulvestrant in patients with hormone receptor-positive advanced breast cancer. San Antonio Breast Cancer Symposium; San Antonio, TX. Dec 10–14; 2013; 2013. p. Abstract PD1-3

28. Janku F, Juric D, Cortes J, Rugo H, Burris HA, Schuler M, Deschler-Baier B, Middleton MR, Gil-Martin M, Berlin J, Winer E, Bootle D, Blumenstein L, Demanse D, Coughlin C, Quadt C, Baselga J. Phase I study of the PI3Kα inhibitor BYL719 plus fulvestrant in patients with PIK3CA-altered and wild type ER+/HER2- locally advanced or metastatic breast cancer. J Clin Oncol. 2014:Abstract PD5-5.
29. Mayer IA, Abramson VG, Isakoff SJ, Forero A, Balko JM, Kuba MG, Sanders ME, Yap JT, Van den Abbeele AD, Li Y, Cantley LC, Winer E, Arteaga CL. Stand up to cancer phase Ib study of pan-phosphoinositide-3-kinase inhibitor buparlisib with letrozole in estrogen receptor-positive/human epidermal growth factor receptor 2-negative metastatic breast cancer. J Clin Oncol. 2014; 32:1202–1209. [PubMed: 24663045]
30. Fu X, Creighton CJ, Biswal NC, Kumar V, Shea M, Herrera S, Contreras A, Gutierrez C, Wang T, Nanda S, Giuliano M, Morrison G, Nardone A, Karlin KL, Westbrook TF, Heiser LM, Anur P, Spellman P, Guichard SM, Smith PD, Davies BR, Klinowska T, Lee AV, Mills GB, Rimawi MF, Hilsenbeck SG, Gray JW, Joshi A, Osborne C, Schiff R. Overcoming endocrine resistance due to reduced PTEN levels in estrogen receptor-positive breast cancer by co-targeting mammalian target of rapamycin, protein kinase B, or mitogen-activated protein kinase kinase. Breast Cancer Res. 2014; 16:430. [PubMed: 25212826]
31. Osborne CK, Wakeling A, Nicholson RI. Fulvestrant: an oestrogen receptor antagonist with a novel mechanism of action. Br J Cancer. 2004; 90(Suppl 1):S2–6. [PubMed: 15094757]
32. Patani N, Dunbier AK, Anderson H, Ghazoui Z, Ribas R, Anderson E, Gao Q, A'Hern R, Mackay A, Lindemann J, Wellings R, Walker J, Kuter I, Martin LA, Dowsett M. Differences in the transcriptional response to fulvestrant and estrogen deprivation in ER-positive breast cancer. Clin Cancer Res. 2014; 20:3962–3973. [PubMed: 24916694]
33. Hall JM, McDonnell DP. The estrogen receptor beta-isoform (ERbeta) of the human estrogen receptor modulates ERalpha transcriptional activity and is a key regulator of the cellular response to estrogens and antiestrogens. Endocrinology. 1999; 140:5566–5578. [PubMed: 10579320]
34. Garcia-Garcia C, Ibrahim YH, Serra V, Calvo MT, Guzman M, Grueso J, Aura C, Perez J, Jessen K, Liu Y, Rommel C, Tabernero J, Baselga J, Scaltriti M. Dual mTORC1/2 and HER2 blockade results in antitumor activity in preclinical models of breast cancer resistant to anti-HER2 therapy. Clin Cancer Res. 2012; 18:2603–2612. [PubMed: 22407832]
35. Nelson JD, Denisenko O, Bomsztyk K. Protocol for the fast chromatin immunoprecipitation (ChIP) method. Nat Protoc. 2006; 1:179–185. [PubMed: 17406230]
36. Toska E, Campbell HA, Shandilya J, Goodfellow SJ, Shore P, Medler KF, Roberts SG. Repression of transcription by WT1-BASP1 requires the myristoylation of BASP1 and the PIP2-dependent recruitment of histone deacetylase. Cell Rep. 2012; 2:462–469. [PubMed: 22939983]
37. Geiss GK, Bumgarner RE, Birditt B, Dahl T, Dowidar N, Dunaway DL, Fell HP, Ferree S, George RD, Grogan T, James JJ, Maysuria M, Mitton JD, Oliveri P, Osborn JL, Peng T, Ratcliffe AL, Webster PJ, Davidson EH, Hood L, Dimitrov K. Direct multiplexed measurement of gene expression with color-coded probe pairs. Nat Biotechnol. 2008; 26:317–325. [PubMed: 18278033]
38. Prat A, Parker JS, Karginova O, Fan C, Livasy C, Herschkowitz JI, He X, Perou CM. Phenotypic and molecular characterization of the claudin-low intrinsic subtype of breast cancer. Breast Cancer Res. 2010; 12:R68. [PubMed: 20813035]
39. Hu Z, Fan C, Livasy C, He X, Oh DS, Ewend MG, Carey LA, Subramanian S, West R, Ikpatt F, Olopade OI, van de Rijn M, Perou CM. A compact VEGF signature associated with distant metastases and poor outcomes. BMC Med. 2009; 7:9. [PubMed: 19291283]
40. Tusher VG, Tibshirani R, Chu G. Significance analysis of microarrays applied to the ionizing radiation response. Proc Natl Acad Sci U S A. 2001; 98:5116–5121. [PubMed: 11309499]
41. Subramanian A, Tamayo P, Mootha VK, Mukherjee S, Ebert BL, Gillette MA, Paulovich A, Pomeroy SL, Golub TR, Lander ES, Mesirov JP. Gene set enrichment analysis: a knowledge-based approach for interpreting genome-wide expression profiles. Proc Natl Acad Sci U S A. 2005; 102:15545–15550. [PubMed: 16199517]

42. Hurtado A, Holmes KA, Ross-Innes CS, Schmidt D, Carroll JS. FOXA1 is a key determinant of estrogen receptor function and endocrine response. Nat Genet. 2011; 43:27–33. [PubMed: 21151129]

43. Gozgit JM, Pentecost BT, Marconi SA, Ricketts-Loriaux RS, Otis CN, Arcaro KF. PLD1 is overexpressed in an ER-negative MCF-7 cell line variant and a subset of phospho-Akt-negative breast carcinomas. Br J Cancer. 2007; 97:809–817. [PubMed: 17726467]

44. van 't Veer LJ, Dai H, van de Vijver MJ, He YD, Hart AA, Mao M, Peterse HL, van der Kooy K, Marton MJ, Witteveen AT, Schreiber GJ, Kerkhoven RM, Roberts C, Linsley PS, Bernards R, Friend SH. Gene expression profiling predicts clinical outcome of breast cancer. Nature. 2002; 415:530–536. [PubMed: 11823860]

45. Doane AS, Danso M, Lal P, Donaton M, Zhang L, Hudis C, Gerald WL. An estrogen receptor-negative breast cancer subset characterized by a hormonally regulated transcriptional program and response to androgen. Oncogene. 2006; 25:3994–4008. [PubMed: 16491124]

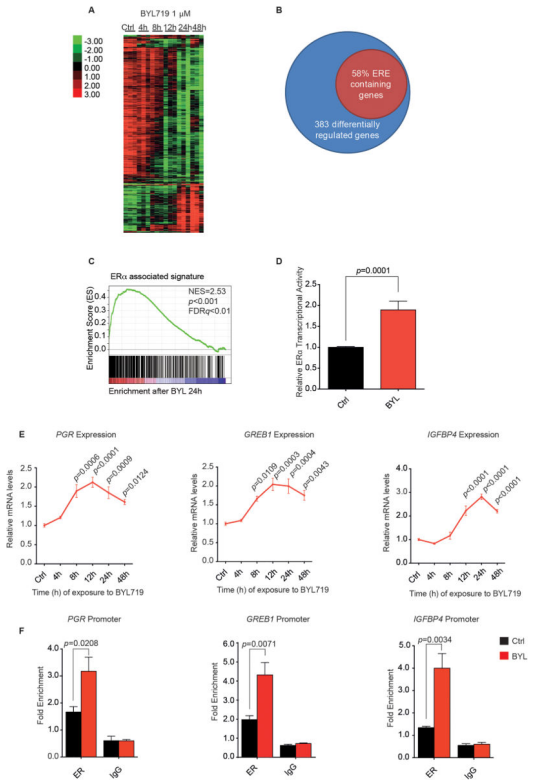

Figure 1. PI3K inhibition promotes ER function

A) MCF7 cells were treated with BYL719 1 μM over a period of 48 hours. RNA was isolated at specified time points and expression microarray analysis performed. Heat map represents genes whose expression differed significantly across different time points with a FDR ≤ 1%. Each of the columns under the experimental conditions represents one biological replicate. B) PI3Kα inhibition leads to modulation of genes containing ER binding sites (ERE). MCF7 cells were treated with BYL719 1 μM, and gene expression analysis was performed as described in A. The diagram represents the genes that were differentially regulated upon treatment across all the time points (SAM analysis FDR ≤ 1%) and the percentage of these genes that contained an ER-binding element (defined by ER ChIP-sequencing (42)). C) GSEA analysis was performed to determine which gene sets were enriched in our data set (FDR ≤ 25%). Graph represents enrichment for ER-associated signature as described in (43). D) MCF7 cells were transfected with firefly- 3X ERE TATA luc and pRL-TK Renilla plasmids, and treated with vehicle (Ctrl) or BYL719 1 μM for 16 hours. Results represent firefly-luciferase activity measured by luminescence and normalized both to renilla-luciferase luminescence for transfection efficiency and to Ctrl. Two-tailed Student's unpaired t test was performed to compare Ctrl *vs* BYL-treated cells. E) MCF7 cells were treated with BYL719 1 μM over a period of 48 hours, and RNA was isolated at the indicated times. qPCR was performed to detect *βACTIN, PGR, GREB1, and IGFBP4* gene expression. The data are presented relative to *βACTIN* and to expression in vehicle-treated cells (Ctrl). One-way ANOVA statistical test was used to compare gene expression between each time point and vehicle-treated cells, applying the Bonferroni method to correct for multiple comparisons. Error bars denote the SEM of at least two

biological replicates, each with three technical replicates. F) MCF7 cells were treated with BYL719 1 μM (BYL) or vehicle (Ctrl), and ChIP was performed with anti-ERα antibody or control IgG. Primers to amplify the ER-binding regions of the *PGR*, *GREB1*, *and IGFBP4* promoters were used in qPCR to determine fold enrichment relative to a noncoding region. Two-tailed Student's unpaired t test was performed to compare Ctrl vs. BYL-treated cells. Error bars represent the standard error of the mean (SEM) of three independent experiments.

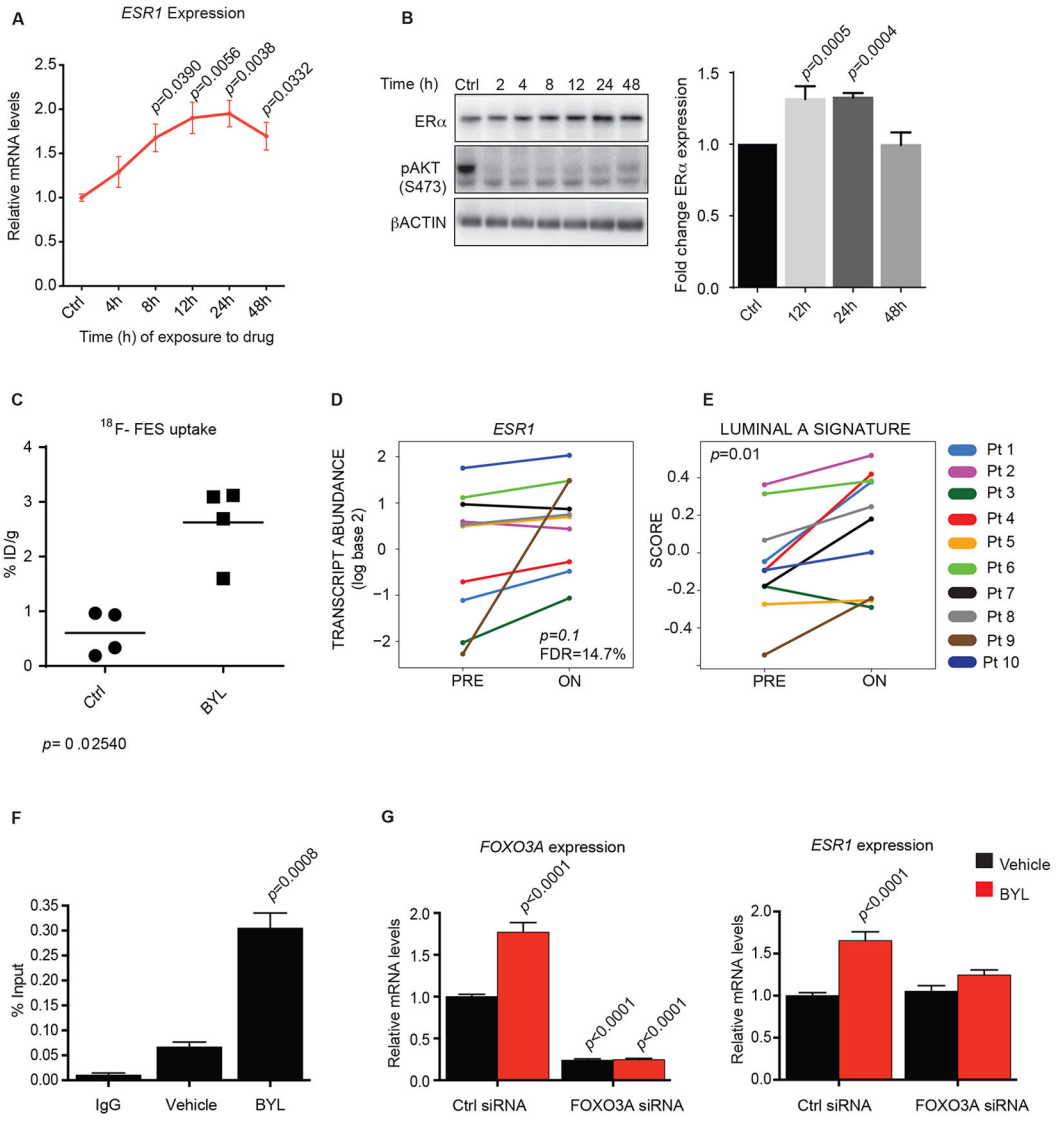

Figure 2. PI3K inhibition induces ER expression

A) MCF7 cells were treated with BYL719 1 μM over a 48 hour period, and RNA was isolated at the indicated times. qPCR was performed to detect *βACTIN* and *ESR1* expression. The data are presented relative to *βACTIN* and to expression of *ESR1* in vehicle-treated control (Ctrl). One-way ANOVA statistical test was used to compare gene expression between each time point and to vehicle-treated cells, applying the Bonferroni method to correct for multiple comparisons. Error bars denote the SEM of at least two biological replicates, each with three technical replicates. B) MCF7 cells were treated with BYL719 1 μM over a period of 48 hours, and total protein was isolated at the indicated times. Immunoblotting was performed to detect expression of ER, phosphorylation of AKT at serine 473 (pAKT S473), and βACTIN. Graph represents the fold change of total ERα with respect to βACTIN and to untreated samples (Ctrl) of two independent experiments. Statistical analysis was done using the one-way ANOVA statistical test with the Bonferroni method to correct for multiple comparisons. C) 16α-^{18}F-fluoro-17β-estradiol (^{18}F-FES)

uptake in T47D xenograft mouse models treated with vehicle or BYL719 daily. The uptake was measured after a 4 day treatment, 2 hours after the last dose, and is represented as % injected dose per gram of tumor tissue (%ID/g). Statistical analysis to compare ^{18}F-FES uptake between the Ctrl and the BYL-treated mice was performed by means of a non-parametric Kruskal-Wallis test. D) Graphical representation of *ESR1* transcript abundance in twenty paired breast cancer biopsies before (PRE) and on BYL719 treatment (ON) collected as part of two clinical trials with the p110α inhibitor BYL719. *ESR1* was one of the 105 breast cancer-specific genes analyzed using the nCounter platform. E) Graphical representation of the induction of a luminal A signature upon BYL719 treatment in the tumor samples used in figure 2D. F) MCF7 cells were treated with vehicle or BYL719 1 μM for 2 hours. ChIP was performed with anti-FOXO3A antibody or control IgG. Primers to amplify the FOXO3A-binding regions of the *ESR1* promoter were used in qPCR to determine fold enrichment relative to input. Two-tailed Student's unpaired t test was performed to compare mean signal amplification between vehicle and BYL719-treated samples. Error bars represent the standard error of the mean (SEM) of two independent experiments with three technical replicates each. G) MCF7 cells were transfected with non-targeted siRNA (Ctrl) or FOXO3 siRNA. Forty-eight hours later, cells were treated with vehicle or BYL719 1 μM for 24 hours. mRNA was isolated, and qPCR was performed to detect *βACTIN*, *FOXO3A*, and *ESR1* expression. The data are presented relative to *βACTIN* and to expression in the samples treated with Ctrl siRNA and vehicle. One-way ANOVA statistical test was used to compare gene expression between each condition and Ctrl siRNA and vehicle-treated cells, applying the Bonferroni method to correct for multiple comparisons. Error bars denote the SEM of two independent experiments with three technical replicates each.

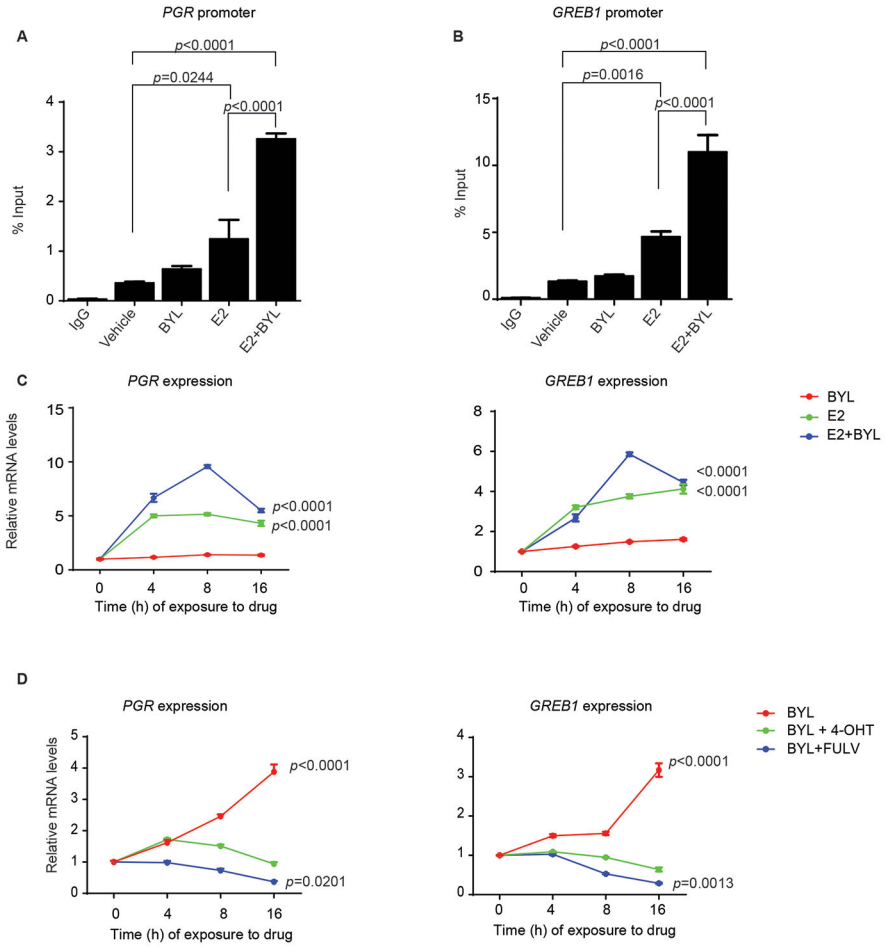

Figure 3. PI3K inhibitor-mediated induction of hormone signaling is dependent on E2 and ER

MCF7 cells were treated with BYL719 1 μM, estradiol (E2) 10 nM, or the combination after 48 hours in estrogen-free medium. ChIP was performed with anti-ERα antibody or control IgG. Primers to amplify the ER-binding regions of the *PGR* (A) and *GREB1* (B) promoters were used in qPCR to determine fold enrichment relative to input. One-way ANOVA statistical test was used to compare mean signal amplification between each treatment and vehicle-treated samples, applying the Bonferroni method to correct for multiple comparisons. Error bars represent the standard error of the mean (SEM) of two independent experiments with three technical replicates each. C) MCF7 cells were pre-incubated for 48 hours in steroid hormone-depleted medium and subsequently treated with BYL719 1 μM, estradiol 10 nM, or the combination over a period of 16 hours, and RNA was isolated at the indicated times. qPCR was performed to detect *βACTIN*, *PGR*, and *GREB1* expression. The data are presented relative to *βACTIN* and to expression at time 0 in the BYL-treated samples. One-way ANOVA statistical test was used to compare gene expression between each treatment and vehicle-treated cells, applying the Bonferroni method to correct for multiple comparisons. The results presented are for the comparisons at the 16 hour time point. Error bars denote the SEM of two independent experiments with three technical replicates each. D) MCF7 cells, grown in normal serum conditions, were treated with BYL719 1 μM, alone or in combination with 4-hydroxytamoxifen 1 μM or fulvestrant 100

nM over a period of 16 hours. mRNA was isolated at the indicated times. qPCR was performed to detect *βACTIN*, *PGR*, and *GREB1* expression. The data are presented relative to *βACTIN* and to expression at time 0 in the vehicle-treated samples. One-way ANOVA statistical test was used to compare gene expression between each treatment and vehicle-treated cells, applying the Bonferroni method to correct for multiple comparisons. The analysis results presented are for the comparisons at the 16 hour time point. Error bars denote the SEM of two independent experiments with three technical replicates each. BYL719 (BYL); estradiol (E2); 4-hydroxytamoxifen (4-OHT); fulvestrant (FULV)

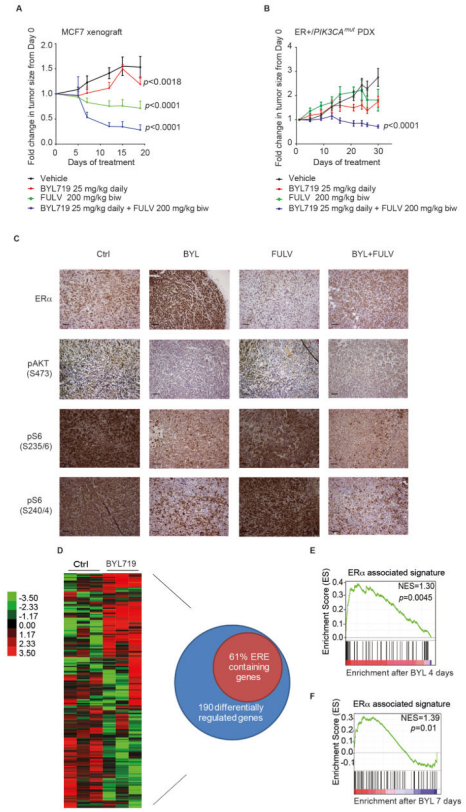

Figure 4. Combination of BYL719 and fulvestrant *in vivo* induces prolonged responses

A) MCF7 *in vivo* xenograft was treated with vehicle, BYL719, fulvestrant, or the combination at the indicated doses and schedule. Graph shows the fold change in tumor volume with respect to day 0 of treatment. One-way ANOVA statistical test was performed to compare tumor volume fold change on the last day of treatment between each treatment arm and vehicle, applying the Bonferroni method to correct for multiple comparisons. Error bars represent standard error of the mean (SEM). B) ER-positive/*PIK3CA*^{mut} patient-derived xenograft (PDX) bearing mice were randomized to receive treatment with indicated doses and schedules of vehicle, BYL719, and/or fulvestrant. Graph shows the fold change in tumor volume with respect to day 0 of treatment. One-way ANOVA statistical test was performed to compare tumor volume fold change on the last day of treatment between each treatment arm and vehicle, applying the Bonferroni method to correct for multiple comparisons. Error bars represent SEM. C) Pharmacodynamic study of MCF7 mouse xenograft. Mice were treated with vehicle, BYL719, fulvestrant, or the combination with the same dosing and schedule as in (A) for 4 days. Animals were sacrificed two hours after the last dose, and tumors processed for immunohistochemistry (IHC) and stained with the indicated antibodies. The figure shows representative images for each of the treatment arms. Scale bars 50 μm. D) A parallel pharmacodynamic study was performed with the ER-positive/*PIK3CA*^{mut} PDX mice, which were treated with either vehicle or BYL719 with the same dosing and schedule as described in (B). Mice were sacrificed and tumors obtained on day 4, 2 hours after the last dose, and processed to obtain RNA for microarray gene expression analysis. Graph represents genes whose expression differed significantly across

different treatments with a FDR ≤ 1%. Each of the columns under the experimental conditions represents one biological replicate. Venn diagram represents differentially regulated genes upon treatment with BYL719 (SAM analysis FDR ≤ 1%) and the percentage of these that contained an ER binding site, defined by ER ChIP-sequencing data available from (42). E) GSEA analysis was performed to determine which gene sets were enriched in the PDX microarray expression data set obtained in (D).Graph represents enrichment for ER-associated signature (FDR ≤ 25%) as described in (44). F) Pharmacodynamic studies on the MCF7 xenografts from (A) were performed on day 7 of treatment, by means of a punch biopsy in both vehicle and BYL-treated mice. A representative number of biopsies (at least two biological replicates per condition) was processed to obtain RNA and submitted for gene expression analysis. GSEA analysis was performed to determine which gene sets were enriched in our data set (FDR ≤ 25%). Graph represents enrichment for ER associated signature as described in (44). Vehicle (Ctrl); BYL719 (BYL); fulvestrant (FULV); combination (BYL+FULV).

Table 1

Differentially expressed genes upon BYL719 treatment in patients with metastatic breast cancer

Paired biopsies of tumors from ER-positive breast cancer patients receiving BYL719 as part of a clinical trial were collected before and during treatment. RNA was extracted, and the expression of 105 breast cancer-specific genes was analyzed using the nCounter platform. Differentially expressed genes (FDR ≤ 25%) between on-treatment and pre-treatment biopsies are shown in the table.

Gene ID	Score (d)	Fold Change	*q*-value (%)
GRB7	2.177	1.273	0.000
BCL2	2.150	1.363	0.000
MDM2	2.046	1.277	0.000
CXXC5	1.770	1.277	11.478
PGR	1.560	1.359	14.667
ESR1	1.452	1.554	14.667
ACTR3B	1.390	1.176	14.667
SFRP1	1.289	1.266	17.742
ERBB2	1.209	1.144	17.742
SLC39A6	1.034	1.140	19.556
PHGDH	0.999	1.253	19.556
FOXA1	0.908	1.103	19.556
FGFR4	0.890	1.269	19.556
GPR160	0.874	1.134	19.556
FOXC1	0.653	1.157	22.564
MLPH	0.641	1.082	22.564
MAPT	0.622	1.124	22.564
BIRC5	−2.009	−1.219	11.478
MYBL2	−1.946	−1.226	11.478
EXO1	−1.544	−1.190	11.478
CENPF	−1.424	−1.202	11.478
CEP55	−1.280	−1.172	11.478
TYMS	−1.276	−1.130	11.478
RRM2	−1.265	−1.208	11.478
CDH3	−1.261	−1.317	11.478
MKI67	−1.227	−1.148	11.478
MELK	−1.164	−1.149	11.478
CCNE1	−1.155	−1.121	11.478
UBE2T	−1.137	−1.131	11.478
KIF2C	−1.111	−1.164	11.478
KNTC2	−1.032	−1.104	11.478
CDCA1	−0.997	−1.130	11.478

Gene ID	Score (d)	Fold Change	*q*-value (%)
ORC6L	−0.988	−1.136	11.478
CDC6	−0.924	−1.143	11.478
CDC20	−0.886	−1.106	11.478
CCNB1	−0.871	−1.093	11.478
PTTG1	−0.759	−1.098	14.667
ANLN	−0.673	−1.096	17.742
MMP11	−0.619	−1.114	17.742